Scientia Iranica B (2022) 29(5), 2349–2361

Sharif University of Technology
Scientia Iranica
Transactions B: Mechanical Engineering
http://scientiairanica.sharif.edu

An investigation into the effective parameters in optimal design of ECAP-Conform process of commercially pure titanium using statistical and numerical approaches

H. Ghaforian Nosrati[a,1], M. Gerdooei[b,*], and K. Khalili[a]

a. *Department of Mechanical Engineering, University of Birjand, Birjand, Iran.*
b. *Faculty of Mechanical and Mechatronics Engineering, Shahrood University of Technology, Shahrood, P.O. Box 3619995161, Iran.*

Received 8 June 2021; received in revised form 31 December 2021; accepted 27 June 2022

KEYWORDS
ECAP-Conform process;
Commercially pure titanium;
Optimization;
Design of experiment;
Finite element method.

Abstract. The Equal Channel Angular Pressing-Conform (ECAP-Conform) process improves the mechanical and functional properties of materials and overcomes the disadvantages of conventional Equal Channel Angular Pressing (ECAP). The main objective of this study is to investigate the variable in the ECAP-Conform process of pure titanium Grade 2. The design of experiments with full factorial technique was implemented in conjunction with finite element numerical simulation. The equivalent plastic strain, required torque, applied force on the ECAP die, and the warping radius of the product were measured, and the results were interpreted using analysis of variance. It was found that the ECAP die angles and the rod bending angle had the highest effect on both imposed strain and required torque. Further, the rod bending angle and the rod-die friction had no significant effect on the warping radius. The optimal values were specified for minimizing the required torque, reaction force, and warping radius and maximizing the imposed strain. Based on the optimal estimated parameters, the minimum values of torque, force, and warping radius and maximum value of equivalent strain were predicted to be 8.4 kN.m, 42 kN, 0.36 m, and 1.7, respectively. Moreover, compared to the case of numerical simulation, the response optimizer obtained the results with less than 8% error.

1. Introduction

In the last decades, Severe Plastic Deformation (SPD) methods have been frequently used to produce Ultrafine-Grained (UFG) materials with unique mechanical and physical properties. This method includes various forming techniques to impose very high strains on materials so as to achieve grain refinement [1]. Among the SPD methods, Equal Channel Angular Pressing (ECAP) has drawn significant attention due to its homogeneous microstructure and a strain of about 1 on each pass through the die [2]. The ECAP process in its original or conventional design is characterized by disadvantages associated with the length of the workpiece: (1) The aspect ratio of the workpiece should be smaller than the critical value which is the reason why buckling does not occur

1. *Present address: Department of Mechanical Engineering, Esfarayen University of Technology, Esfarayen, North Khorasan, Iran.*
*. *Corresponding author. Tel.: +98 23 32392204*
E-mail addresses: h.ghaforiannosrati@gmail.com (H. Ghaforian Nosrati); Gerdooei@shahroodut.ac.ir (M. Gerdooei); kkhalili@birjand.ac.ir (K. Khalili)

doi: 10.24200/sci.2022.58495.5757

and (2) limitation in the stroke of the press ram [3]. Another difficulty that makes this process inefficient due to low production efficiency and high cost is the discontinuity of the process. Also, the length close to each end of the workpiece usually contains a non-uniform structure and can be, therefore, disregarded. Many attempts have been made to overcome these limitations such as Equal-Channel Angular Drawing (ECAD), Accumulative Roll-Bonding (ARB), Repetitive Corrugation and Straightening (RCS), Conshearing, continuous constrained and strip shearing (C2S2), and Equal Channel Angular Pressing Conform (ECAP-Conform) [4]. Volokitina et al. investigated the Finite Element (FE) modeling to combine the ECAP with Drawing processes (ECAP-Drawing) for bimetallic wire deformation. It was found that the stress state of both materials was different in both deformation zones. The deformation in the ECAP zone was divided into sections of tension and compression diagonally, while that in the drawing zone remained completely symmetrical [5]. Krajňák et al. introduced a new SPD technique known as the RCB (Rotational Constrained Bending). They investigated the plastic deformation distribution and microstructure of commercially pure titanium (grade 4). Results demonstrated that the grain size decreased to 400 nm and the tensile strength increased after four passes by about 15% [6]. Another novel technique, which was introduced by Akbarzadeh et al., is the SPD method that Combines the Extrusion and ECAP processes (C-Ex-ECAP). The mentioned authors investigated the microstructural, mechanical, and electrical properties of copper workpieces and found that the yield strength and hardness of samples increased, while electrical conductivity was reduced using this new method [7]. In 1974, Etherington introduced a new idea, Conform, for the continuous extrusion of metals. In this process, wires or powders as feedstock gave rise to the shape of a groove on a roller. Frictional driving force derived from the contact among the three surfaces of the groove with feedstock pushed the feedstock on to outlet. The stationary die covers the groove and causes dragging frictional force by contact interface between the feedstock and stationary die. The cross-section of the outlet usually has a different shape from the groove. Conform process aims to change the geometry of the workpiece or consolidate the powders with only one process pass [8]. The ECAP-Conform process is a combination of the Conform and ECAP processes to produce UFG material continuously. In this process, the stationary constraint dies limit the movement of the workpiece and force them to turn an angle by shear as in a regular ECAP process. In the ECAP-Conform, in addition to the continuous nature of the process, the workpiece plastically bends before entering the shear zone of the die. If the initial cross-section of the workpiece is different from that of the groove cross-section, the ECAP-Conform process will plastically deform the workpiece and match it with the groove cross-section. Figure 1 shows a schematic of ECAP-Conform along with the main characteristic parameters, namely die channel angle (φ), die outer corner angle (ψ), rod bending angle on the roller (α), and warping radius of the formed rod (R).

Raab et al. [4] employed the ECAP-Conform to obtain an UFG commercially pure aluminum wire at room temperature. In their work, the aluminum wire was processed in four passes via ECAP-Conform die at a channel angle of 90°. Their observations showed that after one to two passes, dislocations and low-angle grain boundaries were formed, while after four passes of ECAP-Conform, the grain size of almost 650 nm was obtained. Moreover, the yield strength and the ultimate strength increased by the ECAP-Conform process significantly, while the elongation to failure remained in the range of 12–14%. Subsequently, Raab et al. [9] managed to perform the ECAP-Conform on the Commercially Pure Titanium (CP-Ti) up to 6 passes and reduced the grain size to the range of 200–300 nm. Hoppel et al. [10] used the ECAP-Conform of 6061 aluminum alloy rods and investigated the homogeneity, shear strength, and anisotropy of the product utilizing Vickers microhardness testing.

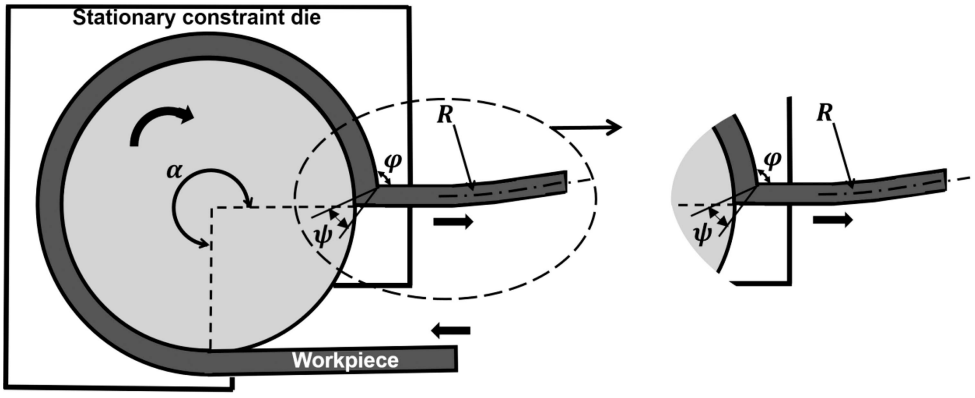

Figure 1. Schematic of the ECAP-Conform process with relevant die parameters.

The results demonstrated that after a single pass, the inhomogeneity of the workpiece increased both on the cross-section plane and longitudinal direction. However, after four passes, distribution of the hardness remained uniformed and the inhomogeneity was significantly reduced. Ayati et al. numerically and experimentally investigated the effect of the groove path of the Conform process on the microstructure and properties of 1100 aluminum. They demonstrated that by increasing the groove path, the strain penetrated to the specimen, which caused non-uniform strain distribution in the deformed sample [11]. In another work, Derakhshan et al. investigated the microstructure of AA 1100 rod and found that after one-pass ECAP-Conform process, the grain sizes remained extremely unchanged and were mostly elongated. On the other hand, the strength of the material increased due to an increase in the dislocation density and formation of subgrains [12]. Mechanical properties and electrical conductivity of Al-Mg-Zr alloy after ECAP-Conform and cold drawing were investigated by Murashkin et al. [13]. Results showed that this process increased the ultimate strength from 129 MPa to 267 MPa accompanied by viable electrical conductivity. Morozova et al. investigated the microstructure of a Cu-0.1%Cr-0.1%Zr alloy after the ECAP-Conform process. It was found that the High-Angle Boundaries (HAB) transformed into Low-Angle Boundaries (LAB) during deformation due to the strain induced by the ECAP-Conform process [14]. Shahab et al. [15] numerically compared the distribution of equivalent plastic strain after continuous confined strip shearing (C2S2) with the ECAP-Conform processes for 1100 Al. The results showed that in the course of the C2S2 process, the sample gradually experienced an equivalent plastic strain of 0.13 at the initial stage of bending, while during the ECAP-Conform process, the strain magnitude of about 0.52 was suddenly imposed. Therefore, the ECAP-Conform process can produce a finer microstructure in the same conditions. The ECAP-Conform process simulation of AA 6061 was performed by Gholami et al. to investigate the effects of die channel angle and friction on the strain and the torque [16]. They examined different channel angles of 90°, 100°, and 110°, in addition to different friction conditions. The results demonstrated that by increasing the channel angle from 90° to 110°, the amount of plastic strain and the required processing torque were reduced by about 40% and 50%, respectively. Besides, greater strain homogeneity was observed at a higher channel angle. Thermo-mechanical ECAP-Conform process of 6082 aluminum was implemented by Procházka et al. [17]. Values of local mechanical properties were estimated by miniaturized tensile testing techniques. The hardness and tensile test results indicated that the microstructure of the samples was subject to inhomogeneity, which was the consequence of the significant strain differences applied to the upper and bottom parts of the aluminum wire. Required torque in the ECAP-Conform process was investigated by Ghaforian Nosrati et al. [18], theoretically and numerically. They calculated the torque of the ECAP-Conform process using the energy balance and the upper-bound methods. In addition, they compared the results of their theory with numerical simulation and observed acceptable compliance. Subsequently, Ghaforian Nosrati et al. performed analytical and experimental studies on the required torque of the ECAP-C process with a square cross-section (for CP-Ti Gr.2). They presented a Slip Threshold Criterion (STC) for performing the ECAP-C process successfully. There was a difference of about 11% between analytical and experimental methods [19].

Nevertheless, the most implemented experimental and numerical studies corresponded to ECAP-Conform of aluminum alloys, and few types of research were carried out on CP-Ti grade 2. Moreover, as can be deduced from the literature, no comprehensive research exists on the evaluation of effective parameters of the ECAP-Conform. Therefore, in the present study, the full factorial Design Of Experiment (DOE) is used to investigate the effect of process parameters such as friction, die angles, and rod bending angle. The response factors include the amount of imposed plastic strain, the required torque, the reaction force, and the warping radius of the product. Finally, the ECAP-Conform machine is manufactured according to the optimal values of these parameters.

2. Materials and methods

2.1. Finite element model

The explicit dynamics procedure in Abaqus/Explicit was used to model the ECAP-Conform process of the CP-Ti grade 2. Figure 2 illustrates the prepared 3D finite element model of this process. The raw material has a circular cross-section of 8 mm diameter and 400 mm length. The material behavior was assumed elastic-plastic, which included density of 4510 kg/m^3, Poisson's ratio of 0.37, and elastic modulus of 105 GPa. The true stress-strain curve of CP-Ti obtained from the compression test according to the ASTM-E9 standard is shown in Figure 3. The CP-Ti rod was deformed by employing a roller with a diameter of 300 mm having a constant rotational velocity of 0.05 rad/s. To reduce the runtime, in addition to employing the mass scaling technique, half of the rod was modeled due to its symmetrical geometry. The contact condition of components was modeled by a surface-to-surface contact along with Coulomb's friction law. The effect of friction condition is considered by employing three different friction coefficients of 0.2, 0.3, and 0.4. According to Figure 2, the symmetrical boundary

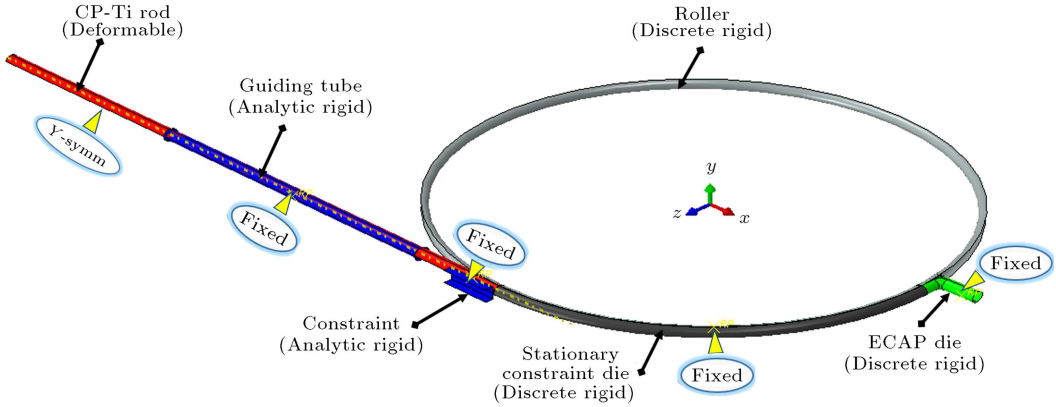

Figure 2. 3D FE model of ECAP-Conform process.

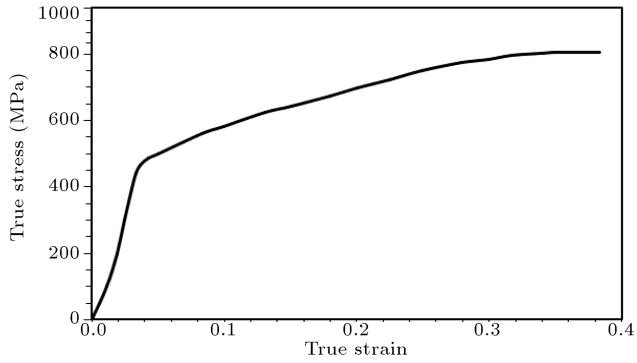

Figure 3. True stress-strain curve of CP-Ti grade 2.

conditions for the rod and fixed reference points for other tools were applied as geometrical constraints in the model. The rod was meshed by using C3D8R (an 8-node linear brick with reduced integration) elements with an optimal element size of 1 mm obtained from mesh sensitivity analysis. Also, the other discrete rigid tools were meshed with R3D4 (4-node 3D bilinear rigid quadrilateral) elements. At the beginning of the simulation, the rod was bitten by the roller due to significant friction between the rod and the groove of the roller. This frictional driving force itself pushed the rod on to the outlet without needing any extra pre-load or mandatory boundary condition.

2.2. Design of experiments

This research aims to understand and predict the effect of the input process parameters on the response of the ECAP-Conform process using a full factorial experiment design. Four independent factors involved friction coefficient between the rod and the roller (μ), the die channel angle (φ), the die outer corner angle (ψ), and the rod bending angle on the roller (α). The four response parameters were equivalent plastic strain (PEEQ), required torque (T), applied reaction force on the ECAP die (F), and warping radius of the formed rod (R). The parameters and their related levels are shown in Table 1. The number of experiments is equal to $3^3 \times 2^1 = 54$.

The maximum amount of required process torque and the maximum applied force to the ECAP die were measured at the reference points of the roller and the die, respectively. Moreover, after exiting the rod from the ECAP die, the maximum effective plastic strain formed at the cross-section of the rod was measured at 20 mm distance from the rod face. Furthermore, as shown in Figure 4, the coordinates of three points with equal distances of 30 mm and sufficient distance from

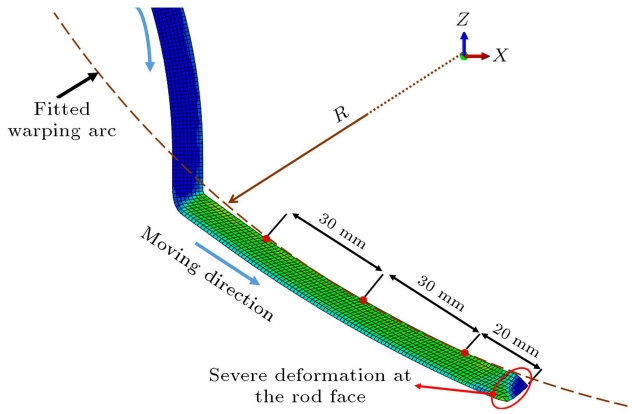

Figure 4. Determining the warping radius of the rod after leaving the ECAP die.

Table 1. Input parameters and related levels for DOE.

Parameter	Level 1	Level 2	Level 3
Friction coefficient between rod and roller (μ)	0.2	0.3	0.4
Die channel angle (φ)	90°	105°	120°
Die outer corner angle (ψ)	0°	30°	60°
Rod bending angle on the roller (α)	60°	90°	–

the rod face were recorded. Finally, by fitting an arc through these three points, the warping radius of the rod was measured.

3. Results and discussion

3.1. Validation of FEM results

To validate the Finite Element Method (FEM) results, a comparison between numerical simulation and theoretical relation for the equivalent plastic strain was conducted. Iwahashi et al. calculated the equivalent plastic strain during ECAP by Eq. (1) [20]:

$$\bar{\varepsilon} = \frac{N}{\sqrt{3}}\left[2cot\left(\frac{\varphi+\psi}{2}\right)+\psi csc\left(\frac{\varphi+\psi}{2}\right)\right], \quad (1)$$

where N is the number of passes and φ and ψ are the die channel and the die outer corner angle, respectively. In addition, the maximum equivalent plastic strain during bending can be calculated through Eq. (2) [21]:

$$\bar{\varepsilon} = \frac{2}{\sqrt{3}}\frac{c}{\rho}, \quad (2)$$

where c and ρ are the radii of the rod and the roller, respectively. The summation of the above-mentioned relations helps determine the total strain of the rod after ECAP-Conform. By incorporating the die channel angles of 90°, 105°, and 120°and $\psi = 30°$ into Eq. (1) and adding $c = 4$ mm and $\rho = 150$ mm to Eq. (2), the imposed strain would be equal to 1.048, 0.838, and 0.655, respectively. In Figure 5, results of the PEEQ at different die channel angles obtained by numerical and analytical methods are compared to one another. It can be seen that at all die channel angles, the analytical method gives a strain smaller than the FEM result. Also, the higher the channel angle, the lower the strain. The difference may result from the failure to consider friction in the simple theoretical approach, which plays a key role in the ECAP-Conform. Similar justifications were also mentioned in other researches [16,20,22].

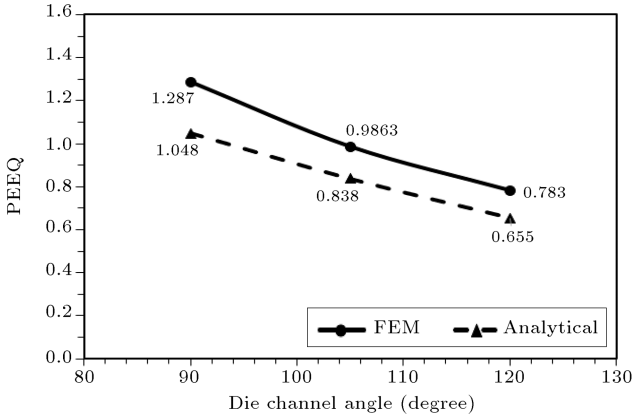

Figure 5. Equivalent plastic strain for different die channel angles obtained by FEM and theoretical methods.

3.2. Analysis Of Variance (ANOVA)

Statistical analysis was carried out to explore the main effects of and interactions between effective parameters during the ECAP-Conform process. The final aim is to determine their optimum range to maximize the imposed strain and minimize required torque and force, in addition to producing a rod with a minimum warping radius. The Analysis Of Variance (ANOVA) method is employed as a useful statistical method to scientifically interpret the interaction between parameters. By investigating the equality of variances and normality distribution of the data, one can deduce that the ANOVA results are valid. Plots of normal probability versus residual and residual versus fitted value will verify these assumptions. Figure 6 shows these plots for one of the responses, namely PEEQ.

Furthermore, the degrees of freedom, the adjusted sum of squares, and mean squares obtained by ANOVA for PEEQ are presented in Table 2. A model is significant in case its P-value is less than 0.05 (by considering a confidence level of 95%). According to the ANOVA table, the die channel angle and the rod bending angle on the roller have the greatest effect among the studied input parameters on PEEQ with 32.86% and 16.47% contributions, respectively. On the other hand, the 2-way and 3-way interactions of input parameters are not significant.

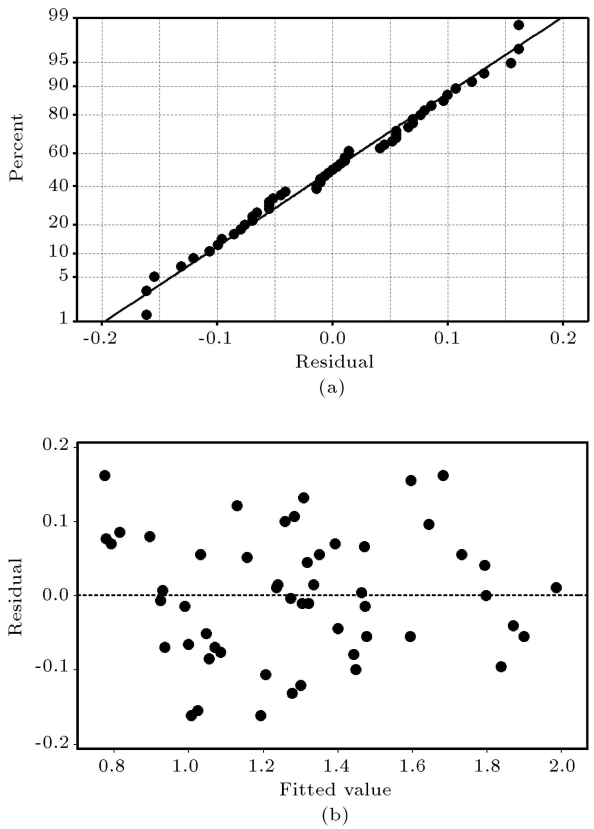

Figure 6. (a) Normal probability plot and (b) residual vs. fitted value plot for PEEQ.

Table 2. ANOVA table for PEEQ.

Source	DF	Seq. SS	Cont. (%)	Adj. SS	Adj. MS	*P*-value
Model	37	4.89308	89.52	4.89308	0.132245	0.006
Linear	7	2.95958	54.15	2.71858	0.388368	0.000
φ	2	1.79591	32.86	1.66666	0.833329	0.000
ψ	2	0.21457	3.93	0.20982	0.104911	0.096
μ	2	0.04916	0.90	0.05935	0.029676	0.477
α	1	0.89995	16.47	0.78944	0.789444	0.000
2-way interactions	18	1.30371	23.85	1.31523	0.073068	0.105
$\varphi \times \psi$	4	0.43450	7.95	0.45545	0.113862	0.054
$\varphi \times \mu$	4	0.24801	4.54	0.23958	0.059894	0.234
$\varphi \times \alpha$	2	0.16668	3.05	0.13793	0.068966	0.198
$\psi \times \mu$	4	0.23067	4.22	0.23391	0.058478	0.243
$\psi \times \alpha$	2	0.21038	3.85	0.15302	0.076509	0.169
$\mu \times \alpha$	2	0.01347	0.25	0.00525	0.002627	0.934
3-way interactions	12	0.62979	11.52	0.62979	0.052483	0.277
$\varphi \times \psi \times \mu$	8	0.33862	6.20	0.34925	0.043656	0.391
$\psi \times \mu \times \alpha$	4	0.29117	5.33	0.29117	0.072792	0.162
Error	15	0.57264	10.48	0.57264	0.038176	–
Total	52	5.46572	100.00	–	–	–

Table 3. AVOVA table for required torque.

Source	DF	Seq. SS $\times 10^8$	Cont. (%)	Adj. SS $\times 10^8$	Adj. MS $\times 10^8$	*P*-value
Model	35	5.3576	93.62	5.3576	0.1530	0.000
Linear	7	3.1786	55.54	3.1879	0.4554	0.000
φ	2	0.3697	6.46	0.4176	0.2088	0.002
ψ	2	0.9785	17.10	1.0253	0.5126	0.000
μ	2	0.4183	7.31	0.3179	0.1589	0.005
α	1	1.4119	24.67	1.4403	1.4403	0.000
2-Way interactions	16	1.3246	23.15	1.3001	0.0812	0.005
$\varphi \times \psi$	4	0.5188	9.07	0.5303	0.1325	0.003
$\varphi \times \mu$	4	0.0216	0.38	0.0263	0.0065	0.870
$\varphi \times \alpha$	2	0.4006	7.00	0.3450	0.1725	0.003
$\psi \times \mu$	4	0.1079	1.89	0.1202	0.0300	0.276
$\psi \times \alpha$	2	0.2755	4.81	0.2629	0.1314	0.010
3-way interactions	12	0.8543	14.93	0.8543	0.0711	0.012
$\varphi \times \psi \times \mu$	8	0.3428	5.99	0.3050	0.0381	0.152
$\varphi \times \psi \times \alpha$	4	0.5114	8.94	0.5114	0.1278	0.003
Error	17	0.3650	6.38	0.3650	0.0214	–
Total	52	5.7227	100.0	–	–	–

Table 3 presents the ANOVA table for the required torque. It is shown that all of the input parameters have a significant effect on the response, while the rod bending angle has the highest effect on the required torque with a 24.67% contribution. Results indicate that some of the 2-way and 3-way interactions of input parameters are not significant. The significant effect of the interaction between die angles and rod bending angle exists. The extent of the contribution in linear, 2-way, and 3-way interactions was 55.54%, 23.15%, and 14.93%, respectively.

The ANOVA table for the applied reaction force is given in Table 4. It is observed that among the investigated factors, die outer corner angle, die channel angle, and rod bending angle have the greatest impact on the reaction force with 29.48%, 13.68%, and 13.27%

Table 4. ANOVA table for reaction force.

Source	DF	Seq. SS $\times 10^{10}$	Cont. (%)	Adj. SS $\times 10^{9}$	Adj. MS $\times 10^{9}$	*P*-value
Model	41	1.6309	90.76	16.3099	0.3978	0.043
Linear	7	1.0596	58.97	10.4282	1.4897	0.001
φ	2	0.2458	13.68	2.0856	1.0428	0.011
ψ	2	0.5298	29.48	4.6753	2.3376	0.001
μ	2	0.0455	2.53	0.4266	0.2133	0.284
α	1	0.2385	13.27	2.1242	2.1242	0.003
2-way interactions	18	0.1514	8.43	1.5239	0.0846	0.867
$\varphi \times \psi$	4	0.0348	1.94	0.3407	0.0851	0.694
$\varphi \times \mu$	4	0.0149	0.83	0.1558	0.0389	0.899
$\varphi \times \alpha$	2	0.0266	1.48	0.2880	0.1440	0.415
$\psi \times \mu$	4	0.0164	0.92	0.0847	0.0211	0.964
$\psi \times \alpha$	2	0.0243	1.35	0.1644	0.0822	0.595
$\mu \times \alpha$	2	0.0342	1.91	0.3892	0.1946	0.314
3-way interactions	16	0.4198	23.36	4.1984	0.2624	0.178
$\varphi \times \psi \times \mu$	8	0.1192	6.64	1.2125	0.1515	0.483
$\varphi \times \psi \times \alpha$	4	0.2751	15.31	2.7602	0.6900	0.020
$\varphi \times \mu \times \alpha$	4	0.0254	1.41	0.2541	0.0635	0.790
Error	11	0.1659	9.24	1.6556	0.1508	–
Total	52	1.7969	100.00	–	–	–

Table 5. ANOVA table for the warping radius of the rod.

Source	DF	Seq. SS	Cont. (%)	Adj. SS	Adj. MS	*P*-value
Model	23	0.937030	95.43	0.937030	0.040740	0.000
Linear	7	0.750429	76.43	0.563856	0.080551	0.000
φ	2	0.573345	58.39	0.478067	0.239034	0.000
ψ	2	0.175974	17.92	0.119056	0.059528	0.000
μ	2	0.000951	0.10	0.000260	0.000130	0.933
α	1	0.000158	0.02	0.000898	0.000898	0.495
2-way interactions	12	0.161890	16.49	0.159905	0.013325	0.000
$\varphi \times \psi$	4	0.113513	11.56	0.091672	0.022918	0.000
$\varphi \times \mu$	4	0.031670	3.23	0.031865	0.007966	0.010
$\varphi \times \alpha$	2	0.012978	1.32	0.016332	0.008166	0.024
$\psi \times \alpha$	2	0.003728	0.38	0.004119	0.002059	0.348
3-way interactions	4	0.024712	2.52	0.024712	0.006178	0.027
$\varphi \times \psi \times \alpha$	4	0.024712	2.52	0.024712	0.006178	0.027
Error	24	0.044822	4.57	0.044822	0.001868	–
Total	47	0.981852	100.00	–	–	–

contributions, respectively. Furthermore, the friction between the roller and the rod as well as the 2-way and 3-way interactions do not have considerable effect on the applied force.

According to Table 5 representing ANOVA for the warping radius, the most important parameters include die channel angle and die outer corner angle with 58.39% and 17.92% contributions, respectively. Moreover, the interaction of these factors ($\varphi \times \psi$) with 11.56% contribution is also significant.

Based on the above-mentioned ANOVA results, the contribution of each process parameter (only the main effects) to the response variables can be summarized, graphically in Figure 7. It was found that the rod bending angle on the roller (α) and the friction coefficient between the rod and the roller (μ) had no effect on the warping radius of the outlet rod. It can be also seen that the die channel angles (φ, ψ) affect all four response parameters. Furthermore, by investigating the aforementioned ANOVA tables, it was

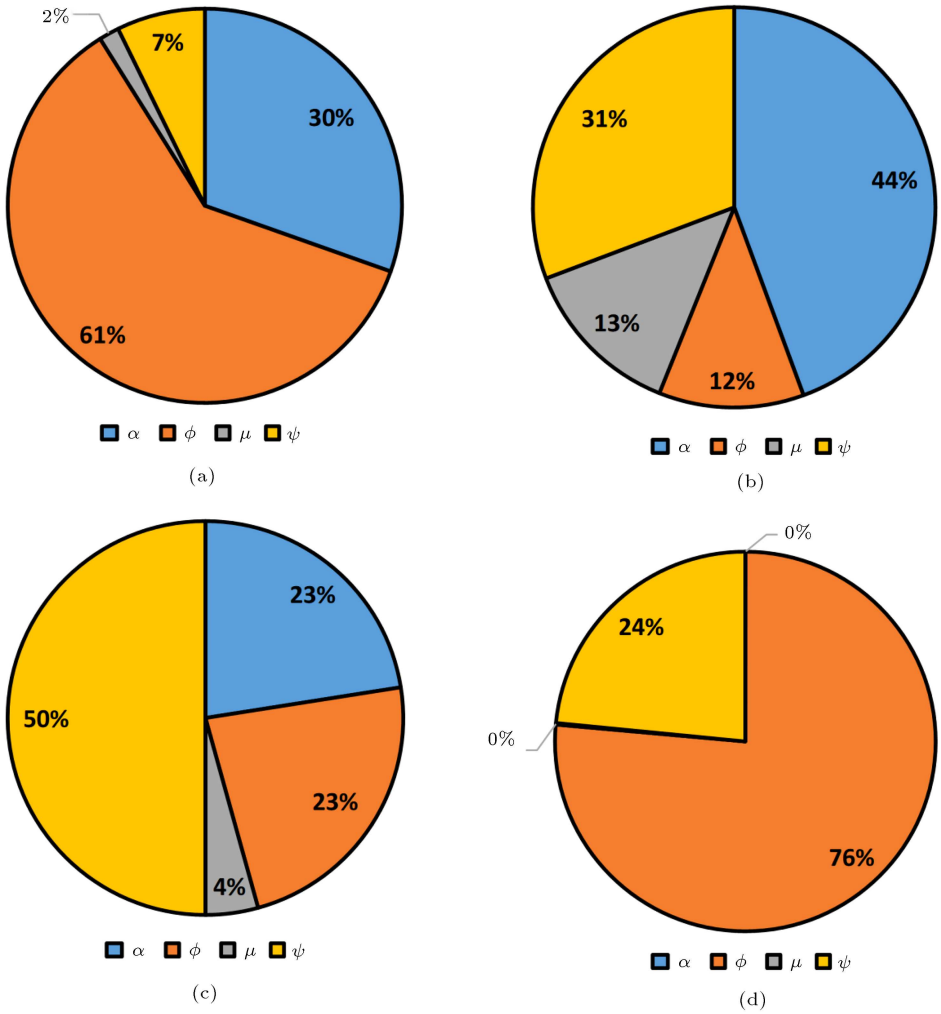

Figure 7. Graphical illustrations for the contribution of process parameters on various responses: (a) PEEQ, (b) required torque (T), (c) force (F), and (d) warping radius (R).

observed that the die channel angle, the die outer corner angle, and the rod bending angle were the three effective factors in the target variables of the ECAP-Conform process. Therefore, the main effects and interactions of these parameters will be evaluated individually in the following sections.

3.3. Main effects

It has been previously stated that the ECAP dies have two effective angles: die channel angle (φ) (usually between 90° to 150°) and die outer corner angle (ψ) (usually in the range of 0° to 90°). Figure 8 shows the main effects of the die channel angle on PEEQ, required torque, reaction force, and the warping radius of the formed rod. Results clearly demonstrate that as the die channel angle increases, the values of all the response parameters decrease.

Similar to the abovementioned procedure, the main effects of the other responses were determined. The outcomes will be discussed briefly and the main effect plots of the other factors are omitted. In the case of the die outer corner angle, the main effect plots indicate that increasing ψ from 0° to 60° can reduce the warping radius by almost 30%. Moreover, by increasing ψ from 0° to 30°, the PEEQ decreases while the reaction force and the required torque increase. However, the above results will be opposite following a great increase in ψ up to 60°. In fact, in this condition, PEEQ increases and the required torque and reaction force are reduced due to the effects of the interaction between parameters.

Based on the main effect plots of the rod bending angle, it can be deduced that when α increases from 60° to 90°, the warping radius and PEEQ of the deformed rod are increased by 1.5% and 18%, respectively. On the other hand, the required torque and the reaction force are reduced.

3.4. Interactions between factors

The interaction between factors appears when the difference in response between the levels of one factor is not the same as that among all levels of other

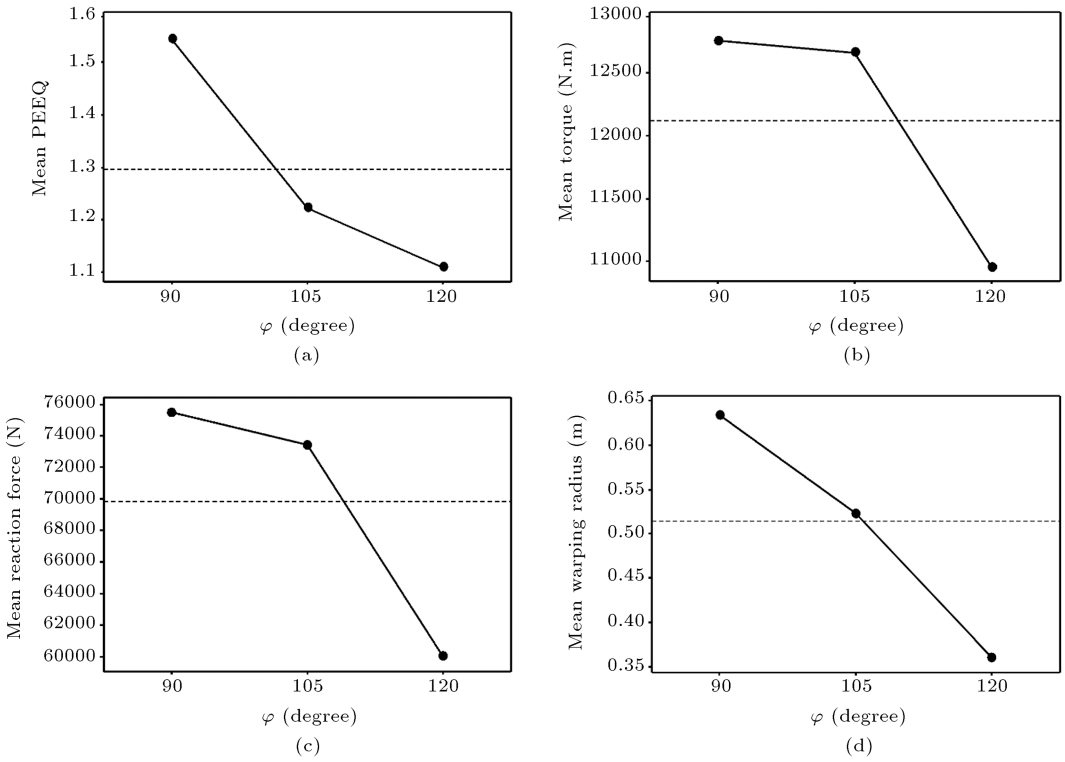

Figure 8. Main effect plots of the die channel angle on (a) PEEQ, (b) required torque, (c) reaction force, and (d) warping radius.

factors [23,24]. If the interaction is significant, the corresponding main effects will be minor. From the ANOVA tables, these effects are recognizable.

Regarding P-values and contribution percentage in ANOVA tables, one can deduce that the interaction among φ, ψ, and α for the required torque (Table 3) should be considered. In addition, at a warping radius, only a 2-way interaction of φ and ψ is important (Table 5). Figure 9 shows the interaction plot of φ, ψ, and α for the required torque. The investigation of these plots along with the ANOVA table of the torque (Table 3) indicates that the contributions for 2-way interactions of $\varphi \times \psi$, $\varphi \times \alpha$, and $\psi \times \alpha$ are 9.07%, 7%, and 4.81%, respectively.

Moreover, the 3-way interaction of $\varphi \times \psi \times \alpha$ has an 8.57% contribution. Therefore, as can be seen in Figure 7, the 2-way interaction of $\varphi \times \psi$ has the highest effect on the response. For the other parameters, 2-way and 3-way interactions do not pose a significant effect; therefore, examining their main effects is necessary and adequate, as mentioned before.

3.5. Optimal levels

The goal of the optimization in the ECAP-Conform process is to minimize the required torque, the reaction force, and the warping radius, in addition to maximizing the amount of imposed equivalent plastic strain after ECAP. In practice, it is not possible to obtain optimal values for all of the responses due to the reverse effects of process parameters on each response. In other words, the improvement of one response has an inevitable negative effect on another. Therefore, the next step is to select the optimal levels to obtain maximum desirability, i.e., all responses achieve an acceptable level of satisfaction. Response optimization can be utilized to find the best combination of parameters that can optimize a single response or a set of responses. For this purpose, the "response optimizer" in Minitab software was employed for this optimality evaluation. Considering the individual and composite desirability, this software selects the best response. The value of desirability takes a range of zero to one; one represents the ideal case. Eq. (3) shows the relation between individual desirability (d) and composite desirability (D):

$$D = (d_1 d_2 \cdots d_m)^{\frac{1}{m}}. \tag{3}$$

Table 6 shows the optimal level for each parameter based on this method.

Regarding all the responses associated with the reported values in Table 6, the overall desirability was achieved as 0.85. Based on the response optimization results, the minimum torque, force, and warping radius obtained by the selected values were predicted to be 8.4 kN.m, 42 kN, and 0.36 m, respectively, while the maximum imposed strain of 1.7 was obtained. Furthermore, the FE simulation of ECAP-Conform

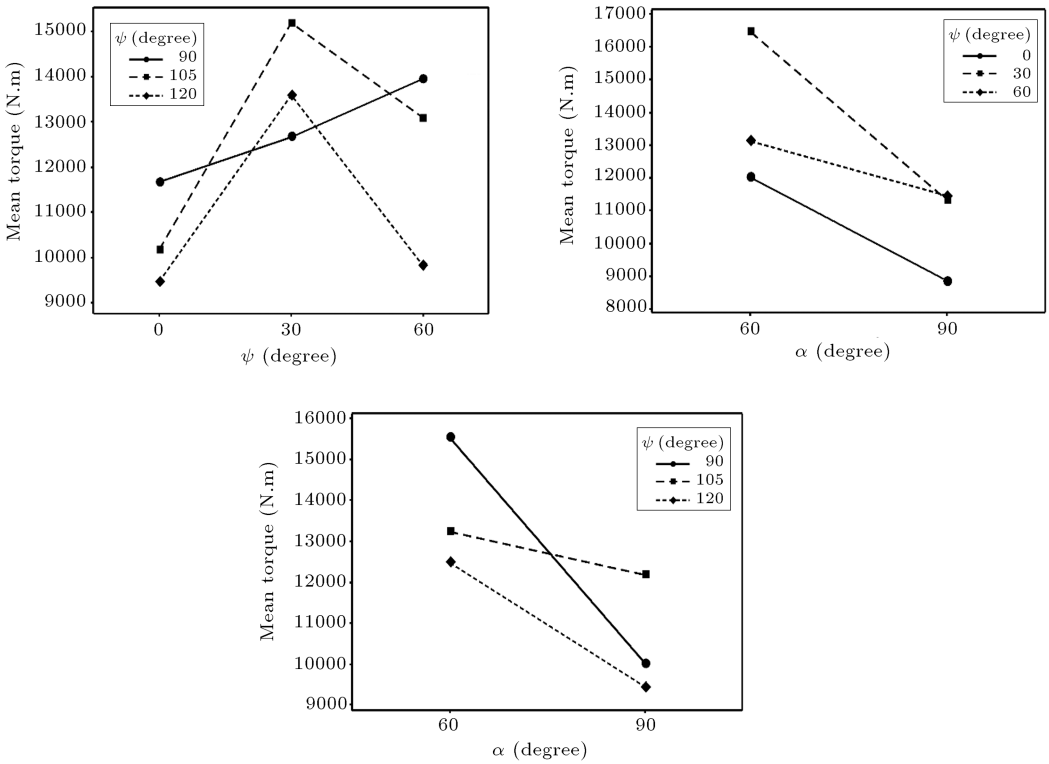

Figure 9. Interaction plots of φ, ψ, and α on the required torque.

Table 6. Optimal values obtained from response optimization.

Parameter	Optimal value	Responses	*d*	*D*
Friction coefficient between rod and roller (μ)	0.2	Required torque (T)	0.84	0.85
Die channel angle (φ)	120°	Reaction force (F)	0.90	
Die outer corner angle (ψ)	0°	Warping radius (R)	0.92	
Rod bending angle on the roller (α)	90°	Equivalent plastic strain (PEEQ)	0.73	

using these optimized values achieved the values of 7.5 kN.m, 36 kN, 0.37 m, and 1.8 for required torque, applied force, warping radius, and PEEQ, respectively.

The mean error in the obtained optimal values is about 8%, compared to the FE simulation. Eq. (4) was used to calculate the error percentage. In this regard, Δ_{Minitab} and Δ_{FE} are Minitab and FE outputs, respectively:

$$\text{Error}\% = \left| \frac{\Delta_{\text{Minitab}} - \Delta_{FE}}{\Delta_{FE}} \right| \times 100. \quad (4)$$

According to the optimal values, the setup of the ECAP-Conform machine was fabricated as shown in Figure 10, and the process was performed for CP-Ti Grade 2. The ECAP-Conform machine was designed with the ability to adjust the roll bending angle (α) from 60° to 270° (by embedding six stationary supports).

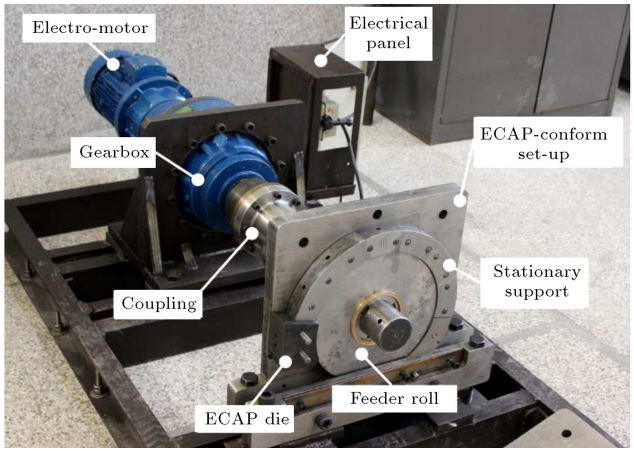

Figure 10. The ECAP-Conform machine.

The microstructure of the as-received CP-Ti and CP-Ti after the one-pass ECAP-Conform process was investigated using the Field Emission Scanning Elec-

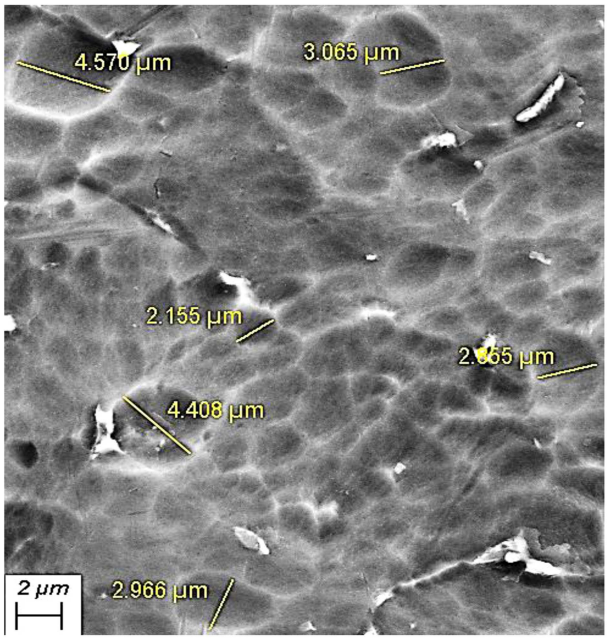

(a)

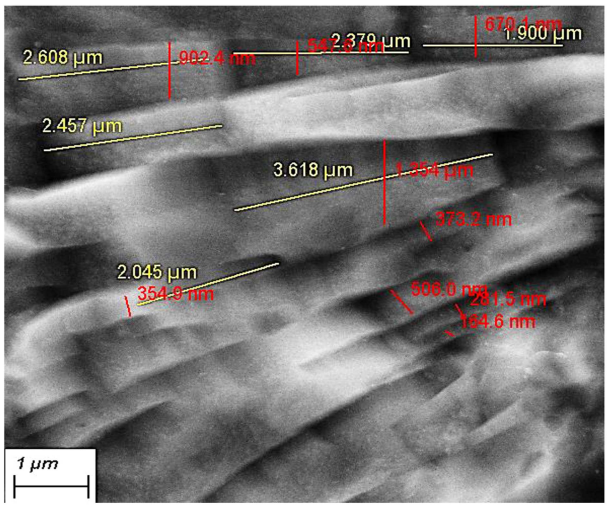

(b)

Figure 11. The FESEM images of CP-Ti rod for (a) as-received specimen and (b) after one-pass ECAP-Conform.

tron Microscope (FESEM). First, samples were cut perpendicular to the direction of ECAP-Conform and after cold mounting, their surface was polished. Then, to clarify the grain boundary, samples were etched up to 140 seconds in a Kroll solution (1 ml HF + 5 ml HNO_3 + 44 ml H_2O). Figure 11 shows the FESEM images for the as-received CP-Ti and CP-Ti after one-pass ECAP-Conform process. As-received titanium has an equiaxed structure with an average grain size of 4 μm. After performing one pass of the ECAP-Conform process, this structure will be elongated due to SPD. The average grain size of titanium after performing one pass of the ECAP-Conform process is 2.5 μm and 1.3 μm in the longitudinal and transverse directions of the grain, respectively. Indeed, about 67.5% and 37.5% reductions in grain size occur in the transverse and longitudinal directions, respectively.

4. Conclusions

In this research, Finite Element Method (FEM) simulationof ECAP-Conform for CP-Ti grade 2 was conducted, and the effect of process parameters including friction condition, die channel angle, die outer corner angle, and the bending angle was examined on the required torque, reaction force, imposed strain, and warping radius of the specimen at the outlet. The following results are obtained using the statistical analysis of variance:

- Among all the studied parameters, the die channel angle (φ) and the bending angle (α) had the greatest impact on the amount of imposed strain. By increasing φ from 90° to 120°, PEEQ in the outlet cross-section was reduced by about 28%. Moreover, when α increased from 60° to 90°, PEEQ was enhanced by 18%;
- All investigated factors had a significant effect on the required torque; the rod bending angle (α) and the outer corner angle (ψ) had the highest effect on the required torque with 24.67% and 17.1% contributions, respectively;
- The friction coefficient would only influence the required torque significantly and its effect on the other response was negligible;
- ECAP die angles, i.e., φ and ψ, exerted the most effect on the warping radius of the specimen by 58% and 18% contributions. The main effect plot of φ revealed that the higher the channel angle, the lower the warping radius. It should be noted that the 2-way interaction between φ and ψ, had a significant effect with an 11.51% contribution;
- The 2-way and the 3-way interactions of input parameters were not significant for PEEQ and reaction force, although they are important for required torque with 24.31% and 16.77% contributions, respectively;
- The optimal values for friction coefficient, channel angle, outer corner angle, and rod bending angle were 0.2, 120°, 0°, and 90°respectively. The predicted values by these adjusted factors were the required torque 8.4 kN.m, reaction force 42 kN, 0.36 m of warping radius, and 1.7 of imposed strain.

References

1. Shaat, M. "Effects of processing conditions on microstructure and mechanical properties of equal-

channel-angular-pressed titanium", *Mater. Sci. Technol.*, **34**(10), pp. 1149–1167 (2018).

2. Horita, Z., Nemoto, M., and Langdon, T.G. "An investigation of microstructural evolution during equal-channel angular pressing", *Acta Mater.*, **45**(11), pp. 4733–4741 (1997).
3. Frint, S., Hockauf, M., Frint, P., et al. "Scaling up segal's principle of equal-channel angular pressing", *Mater. Des.*, **97**, pp. 502–511 (2016).
4. Raab, G.J., Valiev, R.Z., Lowe, T.C., et al. "Continuous processing of ultrafine grained al by ECAP-conform", *Mater. Sci. Eng. A.*, **382**(1–2), pp. 30–34 (2004).
5. Volokitina, I., Volokitin, A., Naizabekov, A., et al. "FEM-study of bimetalic wire deformation during combined ECAP-drawing", *J. Chem. Technol. Metall.*, **56**(2), pp. 410–416 (2021).
6. Krajňák, T., Janeček, M., Minárik, P., et al. "Microstructure evolution and mechanical properties of CP-Ti processed by a novel technique of rotational constrained bending", *Metall. Mater. Trans. A.*, **52**(5), pp. 1665–1678 (2021).
7. Akbarzadeh, B., Gorji, H., Bakhshi-Jooybari, M., et al. "Investigation of mechanical and microstructural properties of pure copper processed by combined extrusion-equal channel angular pressing (C-Ex-ECAP)", *Int. J. Adv. Manuf. Technol.*, **113**(7–8), pp. 2175–2191 (2021).
8. Etherington, C. "Conform-a new concept for the continuous extrusion forming of metals", *J. Eng. Ind.*, **96**(3), pp. 893–900 (1974).
9. Raab, G.I., Valiev, R., Gunderov, D., et al. "Long-length ultrafine-grained titanium rods produced by ECAP-conform", *Mater. Sci. Forum*, **584–586**, pp. 80–85 (2008).
10. Hoppel, H., Kautz, M., Murashkin, M., et al. "An overview: Fatigue behaviour of ultrafine-grained metals and alloys", *Int. J. Fatigue*, **28**(9), pp. 1001–1010 (2006).
11. Ayati, V., Parsa, M.H., and Mirzadeh, H. "Deformation of pure aluminum along the groove path of ECAP-Conform process", *Adv. Eng. Mater.*, **18**(2), pp. 319–323 (2016).
12. Derakhshan, J.F., Parsa, M.H., and Jafarian, H.R. "Microstructure and mechanical properties variations of pure aluminum subjected to one pass of ECAP-Conform process", *Mater. Sci. Eng. A.*, **747**, pp. 120–129 (2019).
13. Murashkin, M.Y., Medvedev, A.E., Kazykhanov, V.U., et al. "Microstructure, strength, electrical conductivity and heat resistance of an Al-Mg-Zr alloy after ECAP-Conform and cold drawing", *Rev. Adv. Mater. Sci.*, **47**(1–2), pp. 16–25 (2016).
14. Morozova, A., Lugovskaya, A., Pilipenko, A., et al. "Microstructure of a low alloyed Cu-Cr-Zr alloy after ECAP-Conform", *IOP Conf. Ser. Mater. Sci. Eng.*, **1014**, p. 012029 (2021).
15. Shahab, A.R., Akbari Mousavi, S.A.A., Ranjbar Bahadori, S., et al. "The comparison between continuous confined strip shearing (C2S2) and ECAP conform in regard to equivalent plastic strain distribution for Al 1100", *Int. J. Mod. Phys. Conf. Ser.*, **05**, pp. 400–409 (2012).
16. Gholami, J., Pourbashiri, M., and Sedighi, M. "Effect of channel angle and friction in modified ECAP-Conform Process of Al-6061: A numerical study", *Iran. J. Mater. Sci. Eng.*, **12**(4), pp. 71–76 (2015).
17. Procházka, R., Sláma, P., Dlouhý, J., et al. "Local mechanical properties and microstructure of EN AW 6082 aluminium alloy processed via ECAP-Conform technique", *Materials (Basel)*, **13**(11), p. 2572 (2020).
18. Ghaforian Nosrati, H., Khalili, K., and Gerdooei, M. "Theoretical and numerical investigation of required torque in ECAP-Conform process", *Metall. Mater. Trans. B.*, **51**(2), pp. 519–528 (2020).
19. Ghaforian Nosrati, H., Khalili, K., and Gerdooei, M. "Theoretical and experimental evaluation of no-slip feeding condition in ECAP-Conform of a square-section metallic rod", *Int. J. Adv. Manuf. Technol.*, **112**(1–2), pp. 375–385 (2021).
20. Iwahashi, Y., Wang, J., Horita, Z., et al. "Principle of equal-channel angular pressing for the processing of ultra-fine grained materials", *Scr. Mater.*, **35**(2), pp. 143–146 (1996).
21. Marciniak, Z., Duncan, J.L., and Hu, S.J. "6-bending of sheet BT-mechanics of sheet metal forming (second edition)", *Butterworth-Heinemann*, Oxford, pp. 82–107 (2002).
22. Furukawa, M., Horita, Z., Nemoto, M., et al. "Review: Processing of metals by equal-channel angular pressing", *J. Mater. Sci.*, **36**(12), pp. 2835–2843 (2001).
23. Montgomery, D.C., *Design and Analysis of Experiments*, John Wiley & Sons (2017).
24. Freddi, A. and Salmon, M. "Design principles and methodologies: Design of experiment", In *Springer Tracts in Mechanical Engineering*, pp. 127–158 (2019).

Biographies

Hasan Ghaforian Nosrati received his PhD degree from the University of Birjand in 2021. He currently is a University Instructor of Mechanical Engineering at the Esfarayen University of Technology. His main research interests include manufacturing and mechanical engineering. He is the author and co-author of many papers in these fields.

Mahdi Gerdooei received his BS, MS, and PhD degrees from the Amirkabir University of Technology, Tehran, Iran. He currently is an Associate Professor at the Mechanical Engineering Faculty at the Shahrood University of Technology, Semnan, Iran. He has conducted research on materials engineering, manufacturing engineering, and mechanical engineering. Most

of his publications are in the field of advanced metal forming methods such as Severe Plastic Deformation (SPD), hydroforming, Rubber Pad Forming (RPF), Fiber Metal Laminates (FMLs).

Khalil Khalili received his BS degree from the Amirkabir University of Technology, MSc and PhD from the University of Salford-UK, and postdoctoral from the University of Nottingham. He was retired in 2017 and joined the Laboratory for Movement-ETH Zurich for a research project. He is currently an Emeritus Professor at the University of Birjand and an inviting Professor at Institute for Biomedical Engineering-ETH Zurich, Switzerland.